Comparison of Single Well and Double and Triple Coupled Well Quantum–Well Infrared Photodetector Designs

S. W. Kennerly, D. W. Beekman*, J. W. Little*, A. C. Goldberg* and R. P. Leavitt

U.S. Army Research Laboratory
Sensors and Electron Devices Directorate
Adelphi, MD

also with
*University of Maryland
College Park, MD

Abstract

A comparison is presented between three GaAs/AlGaAs quantum–well infrared photodetector (QWIP) designs: the conventional single well and two coupled–well designs, one containing two wells per period and the other three. Three QWIP detector test arrays have the same quantum–well width, barrier thickness, doping density in each well, and a peak wavelength of 8.7 μm. The detector array test structures used edge–coupling to remove the grating or optical coupling structure effects from the detector response characteristics. Extensive temperature, bias and spectral–dependent blackbody response and specific detectivity data are presented. The data show that coupled–well designs offer both higher quantum efficiency and lower dark current than the more conventional single–well QWIP.

1. Introduction

There has been significant interest in the physics, design, and performance of Quantum–Well Infrared Photodetectors (QWIPs) for several years.[1] Excellent thermal imagery produced with QWIP focal plane arrays (FPAs) has been impressive[2] and the wide range of single pixel QWIP designs and their performance have been the subject of much interest. The U.S. Army Research Laboratory (ARL), with its Advanced Sensors Consortium Federated Laboratory partners—Sanders, a Lockheed Martin Company, and the University of New Mexico, is investigating the use of QWIP FPAs as part of the Multi-Domain Smart Sensors (MDSS) Task. MDSS is expected to offer multispectral infrared imagery as part of its final demonstration. Given the ambitious goals of the MDSS program, there is some concern about the lower quantum efficiencies observed in conventional QWIPs and the need for operating temperatures that are lower than alternative technologies can operate at. To address these issues, the alternative QWIP structures being investigated here use designs with two and three closely spaced wells in each period of the quantum–well stack.

---

[1] B. F. Levine, K. K. Choi, C. G. Bethea, J. Walker, and R. J. Malik, *Appl. Phys. Lett.*, **50**, 1092 (1987).

[2] W. A. Beck, J. W. Little, A. C Goldberg, and T. S. Faska, Proc. of Electrochemical Society 1st Intl. Symposium on Long Wavelength Infrared Detectors and Arrays: Physics and Applications, 94-5, 21 (1995).

2. QWIP Design

There are numerous QWIP designs that can yield devices that respond in the infrared. In this study, all three structures used a miniband transport (MBT) design.[3,4] The MBT configuration is shown in the conduction band diagram of figure 1 and consists of doped GaAs quantum wells separated by superlattice barrier regions. The quantum wells are designed to contain a ground state and an excited state with an energy separation appropriate to the desired peak wavelength. The superlattice consists of multiple pairs of thin undoped GaAs wells and $Al_{0.3}Ga_{0.7}As$ barrier layers with all wells containing a single energy level. The AlGaAs superlattice barriers are sufficiently thin to allow interaction of the degenerate single energy levels such that they form a miniband, which serves as a conduction channel for photoexcited electrons.

In this comparison, we produced three detector test arrays, each with the same number of periods, quantum–well width, three–dimensional (3–D) doping density in the quantum well, and superlattice barrier thickness separating the absorbing quantum wells. The coupled–well structures are grown with either one or two additional doped quantum wells separated by a thin AlGaAs layer within each period. Each well has the same 3–D doping density; thus, the two and three–coupled well samples will have 2–D doping densities that are respectively, two and three times that of the conventional single well.

For each design, the GaAs quantum–well widths are 62 Å. For this experiment, the AlGaAs barriers separating the coupled wells have a thickness of 40 Å. The MBT barrier design (on each side of the wells in Figure 1) uses a superlattice barrier made of alternating layers of 34–Å of $Al_{0.30}Ga_{0.70}As$ and 11–Å GaAs wells (10 periods plus an additional 34–Å $Al_{0.30}Ga_{0.70}As$ layer). The total barrier thickness for each structure was 484 Å. The full detector design consists of 50 periods. Each absorbing quantum well is uniformly doped with silicon to a doping level of $4 \times 10^{17}/cm^3$. Doped contact layers above and below the 50 period stack have a doping density of $1 \times 10^{18}/cm^3$.

We calculated the electronic states using Airy function solutions to the Schrodinger equation for the quantum–well structures in a uniform electric field. The details of the calculation, including the treatment of band offset and band nonparabolicity, will be presented elsewhere. As designed, the difference between the ground state and the excited state energies is 142 meV, giving a peak–absorption wavelength of 8.7 μm. The excited–state binding energy (difference in energy between the excited state and the conducting channel) is 12 meV for the single well design.

---

[3] S. W. Kennerly, D. W. Beekman, J. W. Little and A. C. Goldberg, *Comparison of MBT and BTQB Quantum Well Infrared Photodetector Designs,* Proceedings of the IRIS: Detector Specialty Group, Monterey, CA (1997).

[4] T. S. Faska, J. W. Little, W. A. Beck, K. J. Ritter, A. C. Goldberg, and R. Leblanc, in *Innovative Long Wavelength Infrared Detector Workshop,* Pasadena, CA, April 7-9. 1992.

3. Experimental Approach

The GaAs/AlGaAs QWIPs used in this study detect only photons with a polarization component perpendicular to the quantum–well layers. When these devices are used for imaging purposes, they always include an optical–coupling structure, such as a grating, to give normal incidence photons an electric field component with the required polarization. Optical–coupling structures can have sharply peaked spectral efficiencies. Because the measured detector response is actually the convolution of the spectral efficiency of the optical–coupling structure with the spectral response of the quantum well, we made our comparison with an edge–coupled geometry with a flat optical coupling efficiency. Figure 2 is a diagram of this test structure configuration. Although this geometry would not be used for an imaging detector, it does provide good data for this comparison and optimization effort. This sample geometry also has the advantage of being easy to fabricate and mount in cryogenic dewars for measurements.

All three samples were prepared from wafers with the same thickness. Each of the three samples contained an 8 x 8 array of 100–μm test pixels. The front edges were polished to a 45° angle with a precision polisher so that both the angle and the distance from the edge to the first row of detector elements were the same from one sample to the next. The back edges were formed by cleaving the wafer, with each sample having the same distance from the edge to the detector elements. The detector array chip was attached to a 68–pin leadless chip carrier (LCC) with conductive epoxy. A 45° angle, highly reflective turning mirror is placed so that its bottom edge aligns with the top edge (on the 45° facet) of the GaAs wafer. Light that is incident normal to the LCC is reflected by the turning mirror onto the 45° facet of the sample and then refracted onto the array. For our performance comparison, we used detector elements from the same row on each sample.

We have made some effort to minimize the amount of scattered radiation within the GaAs wafer that may add to the response of the detector without being properly accounted for in the analysis. Standard glass laboratory microscope slides, opaque to wavelengths longer than 5 μm, were mounted over the detector array. Additionally, the edges of the sample are treated with an infrared–absorbing material so that photons do not reach the quantum–well stack by scattering or reflecting from the edges of the wafer.

4. Detector Characteristics

Figure 3 shows the spectral response (normalized at their peaks) for all three devices, measured at –2.0 volts bias. Both coupled–well devices both showed peak responses of 8.7 μm, while the single well showed a peak response at 8.9 μm, corresponding to a difference in transition energy of 3 meV. The single, double, and triple well structures showed cutoff wavelengths of 9.3, 9.4, and 9.5 μm, respectively. The most striking difference among the three is the widths of the responses. The single–well response full width at half maximum (FWHM) is 1.0 μm, giving a $\Delta\lambda/\lambda$ of 0.11, which is typical of an MBT QWIP. However, the coupled–well design broadens the response significantly. The FWHM values for the double and triple well samples are more than twice that of the single well sample at 2.0 μm ($\Delta\lambda/\lambda$ = 0.23) and 2.4 μm ($\Delta\lambda/\lambda$ = 0.28), respectively.

Extensive temperature-dependent current versus voltage data for all three structures are shown in figure 4. All data shown are dark currents acquired using a cold shutter with the cold shield to completely

enclose the sample. Over typical bias ranges and all temperatures, the currents from the single well sample exceed those of both coupled–well samples despite the larger 2–D doping and slightly longer cutoff wavelengths in the coupled–well samples. The reason for this reduction in dark current is thought to be due to charge–screening effects in the coupled wells that are not present in the single well.

Photoconductive gain is approximately the probability of a conduction electron moving through the detector structure to an electrical contact. The photoconductive gains are determined from the noise and current-voltage measurements (f/3, 295 K illumination) using the relation:

$$g = \frac{<i_{noise}^2>}{4eI_{DC}\triangle f}$$

where i_{noise} = current noise, e = charge on an electron, I_{DC} = current and Δf = noise measurement bandwidth. For background-limited operation, photoconductive gain affects both signal and noise equally and so does not affect the signal-to-noise ratio (or detectivity). Photoconductive gain data for the three samples are shown in figure 5.

Figure 6 shows the blackbody responsivities for all three samples. Peak responsivities can be determined from the blackbody responsivities and the spectral responses shown in figure 3. Responsivity can be expressed as

$$R = \frac{e\lambda}{hc}\eta_a \varepsilon g$$

where e is the electronic charge, λ is the wavelength, h is Planck's constant, c is the speed of light, η_a is the absorption efficiency, ϵ is the extraction probability, and g is the photoconductive gain. Quantum efficiency is defined as the product of absorption efficiency and extraction probability, and equals the probability of a photon ejecting an electron from the ground state to the conduction channel. Using the peak responsivities, peak wavelengths, and the photoconductive gains (fig. 6), we derived the peak quantum efficiencies shown in figure 7. The quantum efficiencies are not proportional to the number of wells because the coupled–well QWIPs have extraction probabilities lower than the single well QWIP.

The detectivity versus bias for each sample is shown in figure 8. The lower curves show the 78 Kelvin detectivity, while the upper curves are 65–Kelvin detectivities. At 78 K, the coupled–well QWIPs exhibit similar detectivities that are 40% higher those of the conventional single–well QWIP. At 65 K, the higher quantum efficiency coupled–well structures exhibit detectivities that are almost twice that of the single well. We have estimated that the coupled–well detectivities measured at 68 or 69 K would be equal to the single–well detectivity at 65 K.

5. Summary

In the development of QWIP arrays, the goal is always to increase the single pixel signal–to–noise ratio by optimizing the design that enhances quantum efficiency, while maintaining or reducing the dark currents. The comparison presented here provides a single pixel design that demonstrates a substantial improvement in the performance of QWIPs that should translate into improvements in FPA performance. These QWIP designs are no more difficult to grow by conventional molecular beam epitaxy (MBE) and the devices are not more difficult to process. We have shown that the coupled–well design dark currents are 50% to 65% of those for a conventional single well QWIP at the same temperatures and with a cutoff wavelength that is slightly longer. The single well QWIP demonstrates higher blackbody responsivity that is achieved primarily through its higher photoconductive gain and extraction probability. Both the double and triple well QWIP structures show higher absorption quantum efficiencies than the single well. The higher quantum efficiencies and lower dark currents shown here allow the coupled–well QWIPs to achieve the same blackbody detectivity as the single well device at operating temperatures approximately 3° higher. These results should also apply to other QWIP designs that achieve reduced dark currents through reductions in the junction area while maintaining their optical area such as the enhanced QWIP[5] (E–QWIP) and corrugated QWIP (C–QWIP).[6]

In the future, we hope to perform a series of measurements on structures where the coupled–well separation is systematically varied. We also hope to study structures in which the excited–state binding energy is varied.

Acknowledgments

We would like to express appreciation for and acknowledge the assistance of Lisa Lucas and Kim Olver in the fabrication and preparation of these QWIP arrays and test structures.

---

[5] T. R. Schimert, S. L. Barnes, J. M. Lloyd, A. J. Brouns, F. C. Case, P. Mitra and L. Claiborne, *Performance Results For A New 64 x 64 Enhanced QWIP Focal Plane Array*, Proceedings of the IRIS: Detector Specialty Group, Laurel, MD (1995)

[6] K. K. Choi, C. J. Chen, A. C. Goldberg, W. H. Chang and D. C. Tsui, *Performance of corrugated quantum well infrared photodetectors*, SPIE AeroSense, Orlando, FL, 13-17 April 1998.

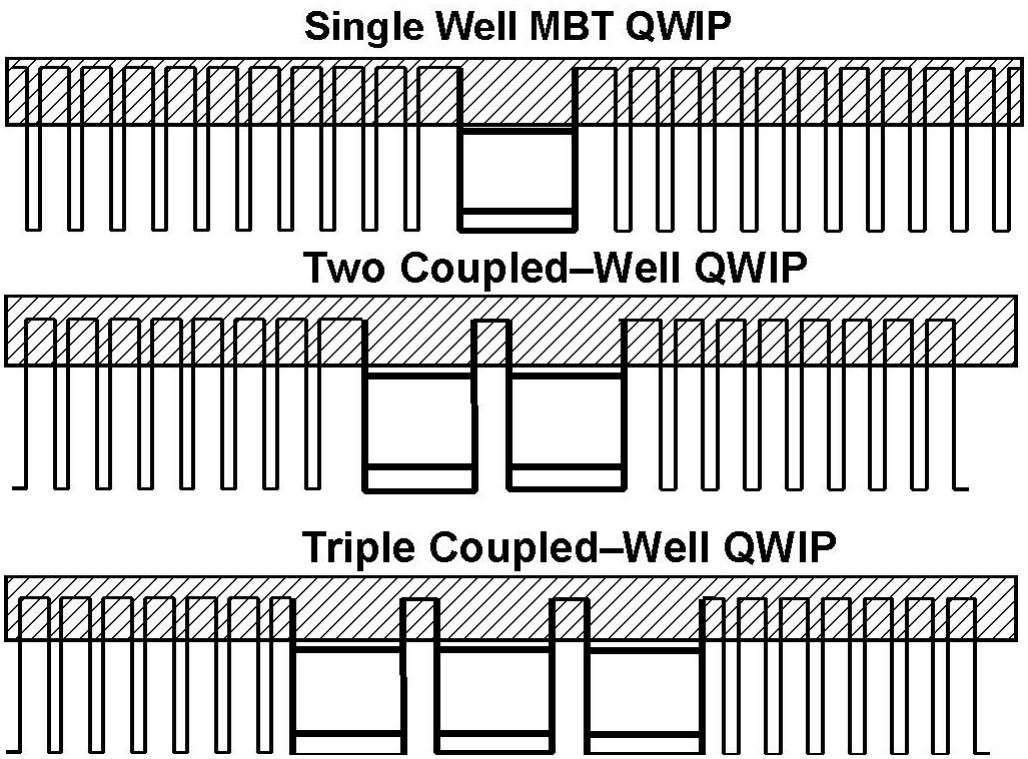

Figure 1: Energy band diagram showing conventional MBT QWIP design and double and triple coupled–well MBT QWIP designs.

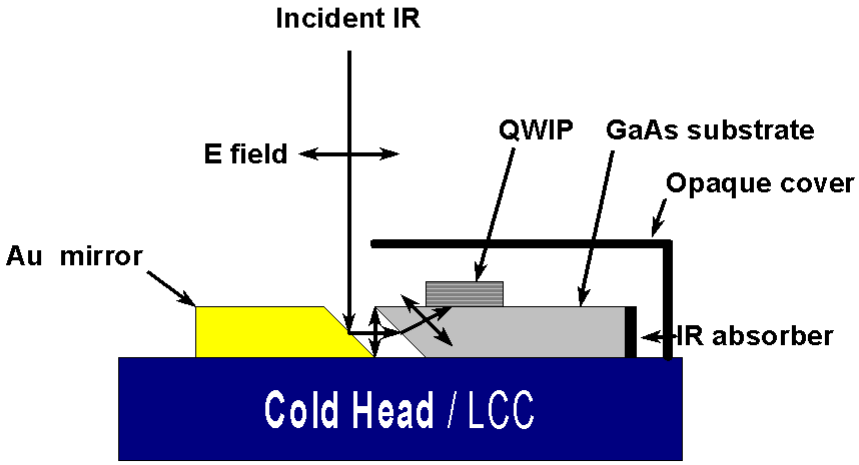

Figure 2: IR detector optical coupling configuration showing 45 degree edges, Au turning mirror, IR absorber, and the opaque glass cover.

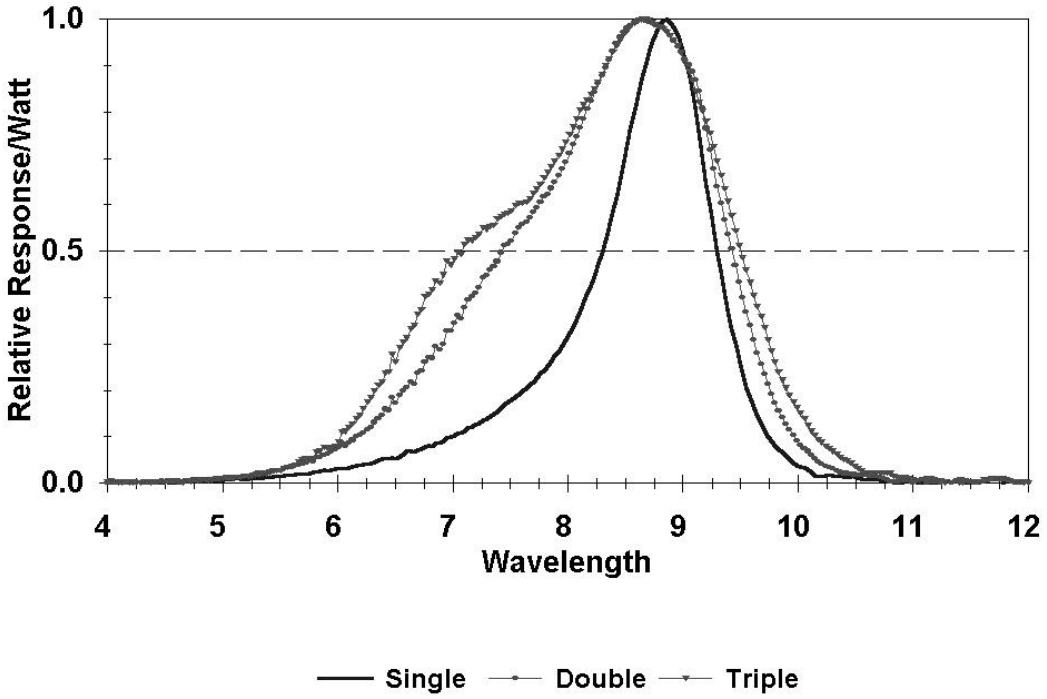

Figure 3: Spectral response for all three QWIP designs, measured at –2.0 volts and 78 Kelvin.

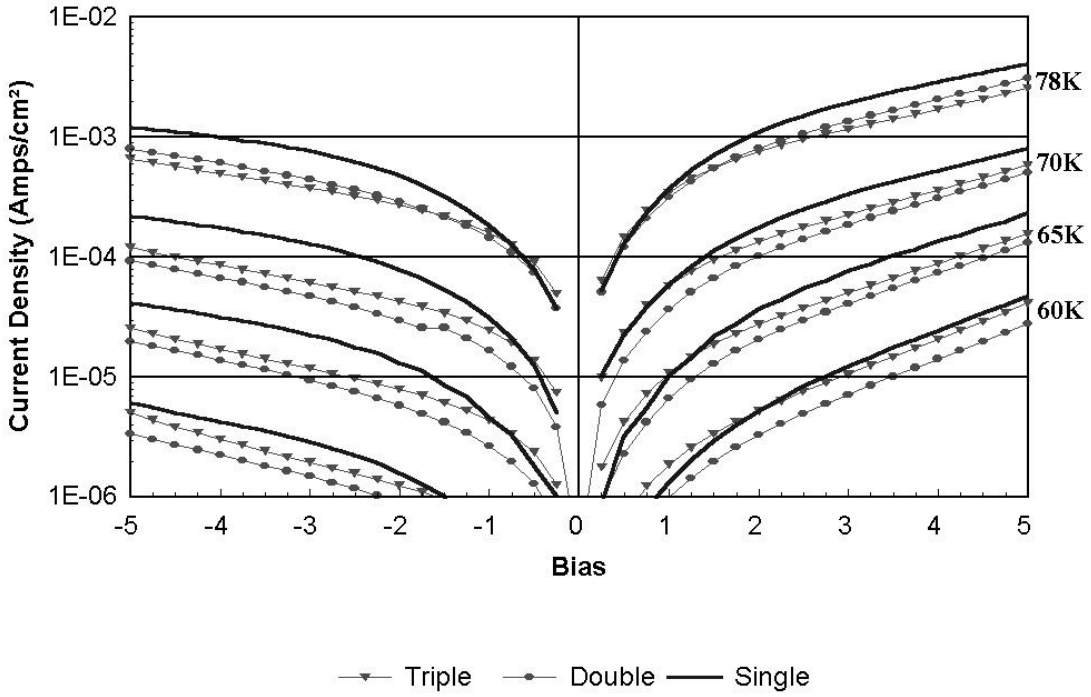

Figure 4: Dark current densities at 60K, 65K, 70K, and 78K for all three QWIP designs.

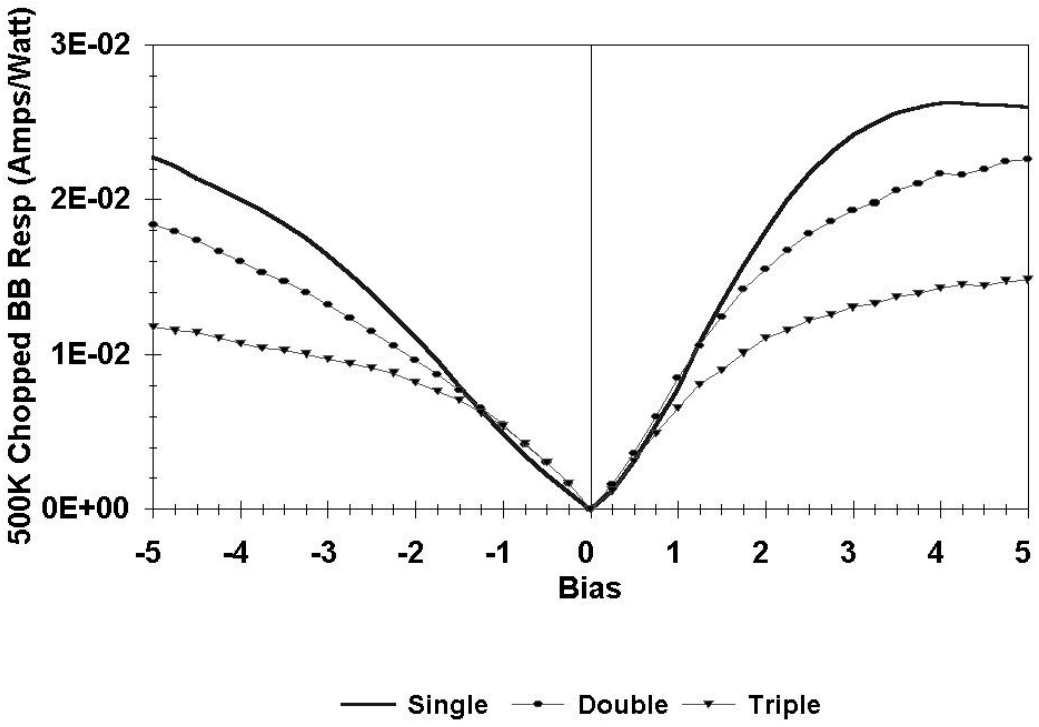

Figure 5: Bias dependence of the 500K chopped blackbody responsivity for all three QWIP designs.

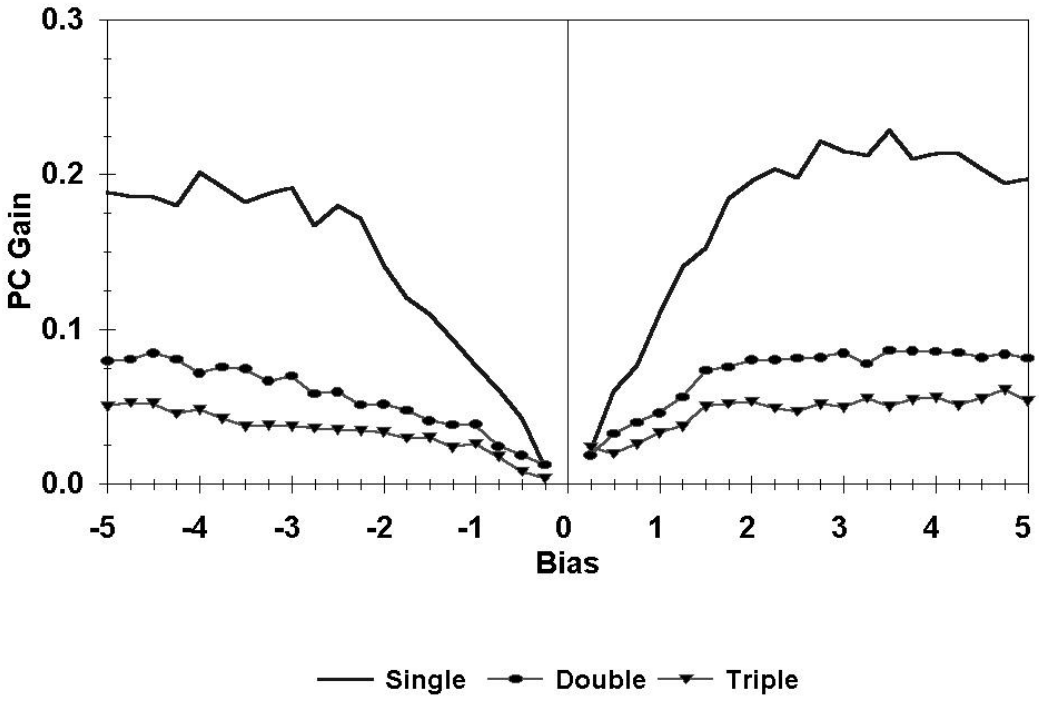

Figure 6: Bias dependence of the photoconductive gains for all three QWIP designs, deduced from IV data and noise data.

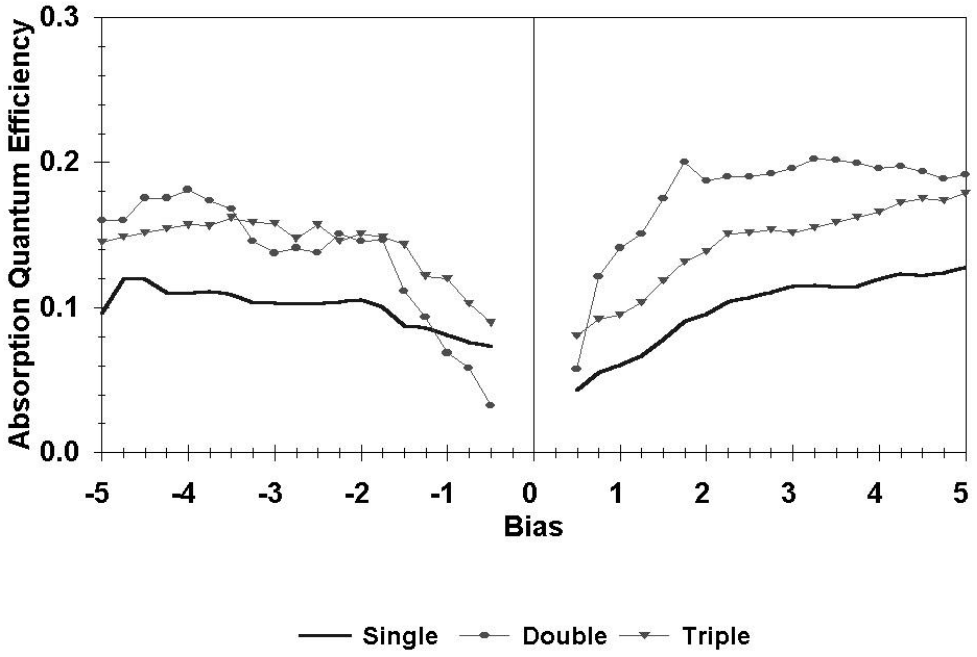

Figure 7: Bias dependence of the absorption quantum efficiency for all three QWIP designs. This absorption quantum efficiency is really the absorption quantum efficiency x extraction probability product.

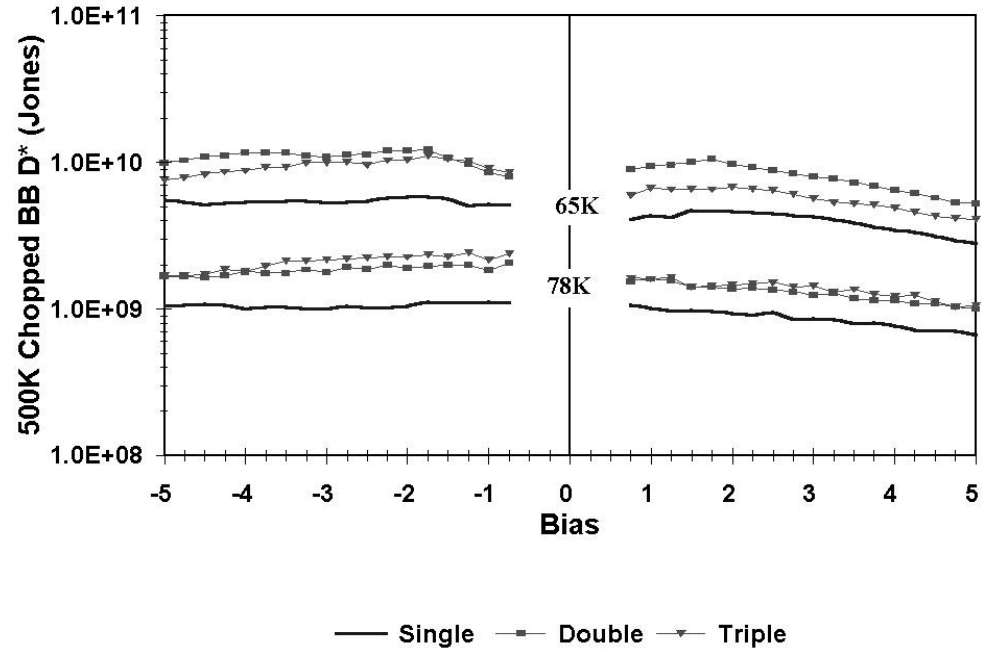

Figure 8: Bias dependence of the 500K chopped blackbody detectivity for all three QWIP designs. The lower three curves are measured at 78K while the three uppermost curves are measured at 65K.